

Sagittal Misalignment Patterns and Pathomechanical Hypothesis of Adolescent Idiopathic Scoliosis: A Radiographic Analysis

Sun Hae (Sunny) Jang¹. Philip Rowe²

Sun Hae (Sunny) Jang
sjang3@emich.edu

Philip Rowe
philip.rowe@strath.ac.uk

1 Orthotics-Prosthetics Master's Program, School of Health Promotion and Human Performance, Eastern Michigan University, Ypsilanti, MI, USA

2 Biomedical Engineering Department, University of Strathclyde, Glasgow, UK

Note: This is the Author Accepted Manuscript (AAM) of an article accepted for publication in Spine Deformity. The final authenticated version of record is available online at: <https://doi.org/10.1007/s43390-025-01268-9>

Abstract

Purpose: This study aimed to identify sagittal misalignment patterns in adolescent idiopathic scoliosis (AIS) by measuring sagittal segmental slope angles of the lower cervical, upper and lower thoracic, and upper and lower lumbar segments relative to the global horizontal line, as well as sagittal deviations of C4, T7, and L3 from the sagittal central sacral line (SCSL) on lateral radiographs of AIS patients. The study also examined the sagittal pathomechanics of AIS, including the compensatory mechanisms underlying these misalignment patterns.

Methods: A retrospective radiographic analysis was conducted using standing full-spine lateral radiographs from 100 AIS patients randomly selected from a scoliosis clinic database. Five sagittal segmental radiographic spinal alignment parameters (RSAPs) and three sagittal deviational angles (SDAs) were measured. Radiographs were classified into distinct sagittal misalignment types based on combinations of SDA values and sagittal segmental RSAP measurements. Statistical analyses were performed to confirm the distinctiveness of each type.

Results: Seven sagittal misalignment types were identified, ranging from **near-normal alignment** to patterns involving mixed combinations of the following features: pronounced posterior tilting of the thoracic spine with excessive posterior decompensation of the superior segments; thoracic hypokyphosis with or without cervical decompensation; vertical straightening of the upper lumbar segments, lower thoracic segments, or both; and lumbar hyperlordosis with **pronounced anterior tilt of the lower lumbar segment**. These profiles reflect regional responses—**anterior displacement or compensatory hyperextension**—to increased extension moments.

Conclusion: AIS sagittal misalignment is driven by **increased extension moments and compensatory hyperextension**, with regional responses governed by **facet joint orientation**. Recognizing these mechanisms supports **universal 3D biomechanical principles** for orthotic design, enhancing sagittal correction and treatment outcomes.

Keywords

Adolescent idiopathic scoliosis, sagittal misalignment, sagittal imbalance, sagittal deformity, extension moment, spinal biomechanics, radiographic analysis, orthotic intervention

Introduction

Adolescent idiopathic scoliosis (AIS) is the most common of the types of idiopathic scoliosis that occurs during the adolescent period. The prevalence of AIS is approximately 2% to 2.5% of most populations, affecting up to 0.15–4% of schoolchildren [1-2]. AIS is a three-dimensional (3D) deformity of the vertebrae, spine, and rib cage that produces asymmetries of the trunk [3]. While the etiopathogenesis is still unknown, it is hypothesized to be multi-factorial [3].

AIS is diagnosed when the spine exhibits more than 10 degrees of coronal curvature with visible rotation on a posterior-anterior (PA) radiograph. Coronal misalignment can be easily

identified by drawing the central sacral line on the radiograph [4]. In contrast, sagittal misalignment has not been well characterized due to the complex, region-specific sagittal architecture of the human spine, which includes kyphotic alignment in the thoracic and sacral regions and lordotic alignment in the cervical and lumbar regions [5-7]. The most well-known sagittal deformity in AIS is the loss of thoracic kyphosis (thoracic hypokyphosis or flattening), particularly when a structural curve is present in the thoracic region. While several classification systems such as the Lenke sagittal modifier and the sagittal classification by Abelin-Genevois et al. have provided valuable insights into sagittal alignment [8-11], they do not fully explain global sagittal misalignment and sagittal imbalance patterns observed in AIS, particularly those relevant to orthotic treatment. Lateral radiographs are often unavailable in smaller orthotic clinics, limiting the ability to assess sagittal plane abnormalities in routine practice. As a result, orthotists frequently rely on assumptions when determining sagittal corrective force placement in 3D orthotic designs, leading to disagreement over universal 3D biomechanical correction principles and contributing to significant variability in the quality of scoliosis orthotic systems [12-16]. In North America, orthotic treatment has also largely relied on manufacturer-specific brace systems such as the Boston Brace, which often do not emphasize sagittal correction, or on European orthotic systems, rather than on the patient-specific 3D deformities of AIS. Therefore, there is an urgent need to more precisely define and classify sagittal misalignment patterns in AIS to establish a foundation for universal 3D orthotic biomechanical correction principles [12].

The Cobb angle method is used to measure thoracic kyphosis and lumbar lordosis curvature on sagittal spine profiles in lateral radiographs. However, it cannot quantify global sagittal alignment, as it only measures angles between two segments. In addition, the normal reference values for the thoracic kyphosis angle and lumbar lordosis angle measured by the Cobb angle

method have never been clearly established. Several studies have been published regarding the normal ranges for the thoracic kyphosis angle and the lumbar lordosis angle, but their reported reference values had ranges that were too wide to be clinically suitable [6, 17-22]. For example, one study found that there was no significant difference in thoracic kyphosis angle and lumbar lordosis angle between the scoliosis group and the non-scoliosis group [20].

The purpose of this study is to identify sagittal misalignment patterns in AIS patients by measuring sagittal slope angles of the lower cervical, upper and lower thoracic, and upper and lower lumbar segments relative to the global horizontal line and spinal deviations of C4, T7, and L3 from the sagittal central sacral line (SCSL) on the lateral view radiographs of AIS spines. Additionally, it examines sagittal pathomechanics of AIS, including its compensatory mechanisms.

Methods

Subject:

This retrospective study utilized lateral view, standing, full-spine radiographs of 100 AIS patients. Subjects were randomly selected from a pool of confirmed AIS patients seen at one of scoliosis clinics in the United States over an eight-year period, as shown in Figure 1. AIS diagnosis criteria included patients aged 10 to 15 years at the time of radiography, Risser value of 0–2, primary curve angle of 20°–50°, and no prior orthotic treatment for scoliosis.

Radiographs were excluded if patients had a leg-length discrepancy >2 cm, lower limb deformities, or had undergone lower limb or spinal surgery, which could contribute to postural scoliosis misdiagnosis. Among each patient's radiograph series, only the first lateral view radiograph, taken at the time of AIS diagnosis and before treatment initiation, was used.

Two Outcome Measures:

a. Sagittal Segmental Radiographic Spinal Alignment Parameters

To quantify the spinal misalignment and deformities of AIS, five sagittal segmental radiographic spinal alignment parameters (RSAPs) were developed based on the segmental slope angles related to the ground which is global horizontal line, and characteristics and biomechanical properties of the non-scoliotic spine. In the non-scoliotic spine, the cervical and lumbar regions are located anterior to the line of gravity (LoG) producing external extension moments whereas the thoracic and sacral regions are placed posterior to the LoG, yielding external flexion moments[23]. This gives the sagittal spinal column a unique alignment, including cervical lordosis, thoracic kyphosis, lumbar lordosis, and sacral kyphosis. Each curvature consists of anteriorly and posteriorly tilted segments, dividing the spine into six segments. The lower cervical, upper thoracic, and lower lumbar segments are anteriorly tilted, producing anteriorly directed shear forces, while the upper cervical, lower thoracic, and upper lumbar segments are posteriorly tilted, generating posteriorly directed shear forces [24-27]. Significant differences in the changes of segmental slope or tilt degrees and direction exist between non-scoliotic and scoliotic spines [24].

Only five of the six spinal segments (the lower cervical, upper thoracic, lower thoracic, upper lumbar, and lower lumbar segments), were of interest in use for developing the parameters for quantifying AIS misalignment because a scoliotic curve does not occur in the upper cervical segment and sacral region.

Based on these sagittal factors, the following five sagittal segmental RSAPs were developed to measure sagittal segmental slope angles related to the global horizontal line for radiographic analysis (Figure 2): *Sagittal Lower Cervical Alignment to Horizontal Angle (SCEA)*; *Sagittal Upper Thoracic Alignment to Horizontal Angle (SUTA)*; *Sagittal Lower Thoracic Alignment to*

Horizontal Angle (SLTA); Sagittal Upper Lumbar Alignment to Horizontal Angle (SULA); Sagittal Lower Lumbar Alignment to Horizontal Angle (SLLA).

b. Three Sagittal Deviational Angles

In addition to the sagittal segmental RASPs, three sagittal deviational angles (SDAs) were also recorded. These angles denoted the deviation of three key anatomical landmarks (C4/5, T7/8, L3/4) of the cervical lordosis, thoracic kyphosis, and lumbar lordosis curvatures from SCSL. The SCSL is defined as a vertical line drawn from the midpoint of the superior endplate of the S1 vertebral body in the sagittal plane, analogous to the coronal central sacral line. In the erect human spine, LoG typically passes near the posterior edges of the C4 and C5 vertebral bodies, anterior to the thoracic spine, and around the posterior edges of the L3 and L4 vertebral bodies. The body's center of gravity lies approximately anterior to the second sacral vertebra (S2), near the center of the pelvis [7]. However, S2 is often difficult to identify on lateral radiographs, whereas the superior endplate of S1 is more consistently visible. Several studies have reported variations in the position of the LoG relative to S1 [23]. Among these, the center of the S1 vertebral body is generally considered the most biomechanically stable reference point, even when excessive sacropelvic anterior tilt is present in AIS.

Figure 3 showed the exact location of each anatomical landmark for the three SDAs and the SCSL. The descriptions of the three SDAs are: *SAC4 (Sagittal Deviational Angle of C4)*: Sagittal deviational angle between the SCSL and the C4/5. This is a sagittal C4 decompensation angle which is represented as a spinal balance; *SAT7 (Sagittal Deviational Angle of T7)*: Sagittal deviational angle measured between the SCSL and the T7/8; *SAL3 (Sagittal Deviational Angle of L3)*: Sagittal deviational angle measured between the SCSL and the L3/4.

If there is no misalignment in the spine, the SAC4 and SAL3 should have close to “zero (neutral)” value while the SAT7 has a positive value. If any key anatomical landmark is located anterior to the SCSL, the measurement was marked as a negative value; if it was located on the SCSL, the measurement was marked as a zero value; and if it was located posterior to the SCSL, it was marked as a positive value.

Data Collection:

The five sagittal segmental RSAPs and three sagittal deviational angles were measured on the lateral view, standing, full-spine radiographs of the AIS patients through the *Carestream Picture Archiving and Communication System (PACS)* digital-imaging program by a single operator.

Data Analysis:

For sagittal misalignment patterns, the 100 lateral view radiographs were categorized into different sagittal misalignment types by grouping combinations of the positive, negative, or zero values of SAC4, SAT7, and SAL3. If any RSAP segments within the same group displayed differences in slope direction—either anteriorly inclined or posteriorly inclined based on RSAP measurements—the radiographs were reclassified into separate groups. The measurements of the five sagittal segmental RSAPs for each sagittal misalignment type were analyzed statistically using descriptive statistics and tests of normality. To verify whether the classified groups represent distinct sagittal alignment types, both parametric tests (two-tailed t-test) and non-parametric tests (two-tailed Mann-Whitney U test) were performed using IBM SPSS Statistics Version 25 (IBM Corporation, Armonk, NY, United States), comparing each group with the one that had the "minimal misalignment" or was the "closest to a neutrally aligned type. Statistical significance for all testing was set with an α of 0.05. To visualize each misalignment type, Microsoft Excel was used to illustrate the sagittal misalignment shapes.

Results

The average age of the 100 randomly selected AIS patients (97 females and 3 males) was 12.6 years old. The distribution of curve patterns was as follows: 46 double thoracic, and lumbar or thoracolumbar curves, 33 single thoracic curves, 15 single lumbar or thoracolumbar curves, 3 triple curves, 2 double two thoracic curves, and 1 double upper thoracic and thoracolumbar curve. The average Cobb angle magnitudes for each curve were $31.8 \pm 5.2^\circ$ for upper thoracic curves, $31.5 \pm 11.8^\circ$ for thoracic curves, and $28.7 \pm 8.4^\circ$ for lumbar or thoracolumbar curves. Seven major sagittal misalignment patterns were identified (Table 1). Table 1 presents the values of the three SDAs and the mean \pm standard deviation for the five sagittal segmental RSAPs for each sagittal misalignment type. Type 1 was defined as minimally misaligned, or the type closest to the natural alignment. All radiographs classified as Type 1 had values of “0” for SAC4 and SAL3, and “+” for SAT7, matching the pattern observed in non-scoliotic spines. The tilt directions of the segments in Type 1 also mirrored those in a non-scoliotic spine, with anteriorly inclined lower cervical (SCEA: 70.1 ± 4.5), upper thoracic (SUTA: 72.9 ± 3.3), and lower lumbar (SLLA: 80.1 ± 5.3) segments, and posteriorly inclined lower thoracic (SLTA: 103.0 ± 4.2) and upper lumbar (SULA: 107.1 ± 3.6) segments.

Other types showed different combinations of SDA values, except for Types 2 and 3. All types included at least one misaligned segment, defined as a segment whose slope direction differed from that of the corresponding segment in the non-scoliotic spine, based on the measured sagittal segmental RSAP values. Although Types 2 and 3 had the same combination of SDA values, they were classified as distinct types because the specific combinations of misaligned segments differed.

Table 1 also showed the results of non-parametric two-sample tests, conducted to determine whether each sagittal misalignment type was statistically distinct. This was done by comparing the mean RSAP values of each type (Types 2-7) to those of Type 1.

Discussion

Seven Sagittal Misalignment Types:

Type 1 represents an idealized reference configuration of sagittal alignment in non-scoliotic spines—characterized by cervical lordosis, thoracic kyphosis, and lumbar lordosis—consistent with the multiple sagittal morphotypes described by Roussouly et al. [28]. This reference served as the baseline for defining the other misalignment types. These patterns exhibited various combinations of the following features: pronounced posterior tilting of the thoracic spine with excessive posterior decompensation of the superior segments; thoracic hypokyphosis with or without cervical decompensation; vertical straightening of the upper lumbar segments, lower thoracic segments, or both; and lumbar hyperlordosis with pronounced anterior tilt of the lower lumbar segment.

Table 2 presents the sagittal segmental misalignment characteristics of each type based on the five sagittal segmental RSAP measurements and SDA values shown in Table 1. In Figure 4, all seven sagittal misalignment patterns are illustrated based on the mean values of the five sagittal segmental RSAPs shown in Table 1. The figure also presents representative radiographic examples of each sagittal misalignment type.

Sagittal Pathomechanics and Compensatory Mechanisms of AIS Deformity:

Alterations in sagittal segmental slope angles relative to the natural alignment of non-scoliotic spines, along with deviations of key anatomical landmarks from the SCSL, are considered to

play an important role in the development and progression of spinal misalignment and imbalance in AIS.

a. Anterior Displacement of the Upper and Lower Lumbar Segments

When misalignment occurs in the upper lumbar segments (Types 3, 4, 5, 6, and 7), the normally posteriorly inclined segments become less posteriorly tilted and more vertically oriented. In contrast, when misalignment involves the lower lumbar segments (Types 5, 6, and 7), the naturally anteriorly inclined segments become more anteriorly tilted.

When both the upper and lower lumbar segments are involved (Types 5–7), the lumbar spine exhibits marked anterior displacement, and L3 shows pronounced anterior deviation from the SCSL. This is accompanied by excessive anterior tilt of the lower lumbar segments and vertical alignment of the upper lumbar segments, leading to the development of severe lumbar hyperlordosis. Given the vertically oriented anatomical structure of the lumbar facet joints, which facilitates anterior translation, this anterior displacement of the lumbar spine appears to be biomechanically plausible [31, 32].

b. Compensatory Hyperextension of Superior Segments (Lower Cervical and Upper Thoracic)

Unlike the lumbar spine, anterior displacement was not observed in the thoracic spine. Instead, in all misalignment types except Type 1, either a relatively greater posterior tilt in the cervical segments, an atypical posterior tilt (rather than the expected anterior tilt) in the upper thoracic segments, or both were observed.

Dickson et al. [29] reported that tightening of the posterior spinal structures in the lower thoracic region occurs in response to anteriorly directed forces at the thoracic apex, resulting in posterior tilting of the upper thoracic spine and reduced thoracic kyphosis. This pattern can

be reasonably attributed to the oblique anatomical orientation of the thoracic facet joints, which restricts anterior translation [31,32].

Based on this framework, reduced thoracic kyphosis (thoracic hypokyphosis) with posterior tilting of the upper thoracic segments, as observed in Types 2–7, and posterior sagittal imbalance (C4 posterior decompensation), particularly evident in Types 2, 3, and 7, are considered manifestations of compensatory hyperextension of the superior segments. This compensatory hyperextension can be interpreted as an equilibrium response to anteriorly directed forces acting on the lower thoracic segment or between the upper and lower thoracic segments.

c. Anterior Displacement or Compensatory Hyperextension of Lower Thoracic Segment

The lower thoracic segment shows variable alignment, exhibiting either anterior displacement similar to the upper lumbar segment or compensatory hyperextension resembling that seen in the upper thoracic or lower cervical segments. In Types 2 and 5, it is more posteriorly tilted than neutral, consistent with compensatory hyperextension. Pronounced posterior tilting of the thoracic spine with marked posterior decompensation of the superior segments is particularly evident in Type 2, which does not exhibit anterior displacement of the lumbar spine.

In contrast, in Type 4, the lower thoracic segment appears vertically straightened, similar to the upper lumbar segment. Consequently, Type 4 produces the most globally straightened sagittal profile among all patterns, through a combination of upper lumbar anterior displacement and upper thoracic compensatory hyperextension, resulting in mild thoracic hypokyphosis and anterior C4 decompensation.

d. Anteriorly Directed Forces Acting on Specific Segments or Between Segments

The origin of the anteriorly directed forces responsible for these deformities remains unknown; however, this study proposes the presence of such forces acting on specific spinal segments. This concept aligns with the biplanar spinal theory proposed by Dickson et al. [29], which describes anteriorly directed mechanical forces acting on the apical vertebral body in the thoracic spine when a thoracic scoliotic curve is present. According to Burwell's aetiological model [30], the thoracic curve in AIS originates in the sagittal plane, producing relatively increased lordosis (or reduced thoracic kyphosis) at the thoracic apex, followed by sequential vertebral rotation in the transverse plane and lateral displacement toward the convex side of the curve.

Although these theories have traditionally been applied to the thoracic apex, the present study extends their relevance to the entire spine, suggesting that similar anteriorly directed forces are present, as evidenced by anterior displacement in the lumbar region and, in some cases, the lower thoracic segment.

e. Increased Extension Moments, Compensatory Mechanisms, and the Development of AIS

Sagittal Misalignment

When anteriorly directed forces act on the spinal column, they generate increased extension moments, which appear to give rise to the diverse sagittal profiles observed in AIS and to distinct segmental responses based on regional anatomy. In the lumbar spine, where vertically oriented facet joints facilitate anterior translation, these forces induce severe anterior displacement of the lumbar spine and significant anterior deviation of the L3 vertebra. This manifestation typically involves marked anterior tilt of the lower lumbar segments, vertical straightening of the upper lumbar segments, or a combination of both, ultimately culminating in severe lumbar hyperlordosis. In contrast, the oblique orientation of the thoracic facet joints

restricts anterior translation; therefore, the superior segments respond to these forces through compensatory hyperextension as an equilibrium response. This response results in atypical posterior tilting of the upper thoracic and/or lower cervical regions (and, in some cases, involves the lower thoracic segment), leading to thoracic hypokyphosis with varying degrees of cervical decompensation. When compensatory hyperextension involves the lower thoracic segment, pronounced posterior tilting of the thoracic spine accompanied by excessive posterior decompensation of the superior segments is observed.

These mechanisms also contribute to vertical straightening of the upper lumbar and/or lower thoracic segments, sometimes producing a globally straightened sagittal profile, while in other cases near-normal sagittal alignment is maintained.

Collectively, these findings indicate that sagittal misalignment in AIS may be fundamentally driven by increased extension moments and compensatory hyperextension of the superior segments acting throughout the spinal column in the sagittal plane. Accordingly, this study further hypothesizes that as the spine undergoes progressive multisegmental misalignment, the spinal column gradually straightens or arches posteriorly, followed by segmental rotation toward the convex side and sequential lateral displacement, consistent with Burwell's aetiological model [30].

Clinical Implications for Orthotic Intervention:

Identifying global sagittal misalignment and imbalance patterns in AIS and understanding how these misalignments contribute to deformity development (pathomechanics), has important clinical implications, particularly for orthotic intervention strategies. This is because the primary goal of orthotic treatment in AIS is to restore the spine to a near-neutral alignment across all three planes, including the sagittal profile. However, sagittal correction has often been

overlooked or applied empirically due to a limited understanding of sagittal misalignment. This study provides a biomechanical foundation for achieving sagittal correction within the orthosis, which may enhance the overall effectiveness of scoliosis treatment.

Limits and Further Directions:

This study has several limitations. The smaller proportion of patients with Types 4–7 reflects their lower prevalence, which may limit the statistical robustness of those subgroups. Second, this study analyzed only sagittal parameters. Because sagittal and coronal alignments are biomechanically interdependent, our ongoing research aims to explore how specific sagittal misalignment patterns correspond to coronal misalignment, including curve magnitude and other misalignment classifications. This may provide a more comprehensive three-dimensional understanding of AIS pathomechanics.

Conclusion

This study identified seven distinct sagittal misalignment and imbalance patterns in AIS, emphasizing the role of anteriorly directed forces and increased extension moments acting on specific spinal segments. These forces cause anterior displacement of inferior segments, specifically the upper and lower lumbar segments and, in some cases, the lower thoracic segment, and compensatory hyperextension of superior segments, including the lower cervical and upper thoracic segments (and, in some cases, the lower thoracic segment). Together, these regional anatomical responses result in a varied range of sagittal profiles, including mixed combinations of pronounced posterior tilting of the thoracic spine with excessive posterior decompensation of the superior segments, thoracic hypokyphosis with or without cervical decompensation, vertical straightening of the upper lumbar and/or lower thoracic segments, and

lumbar hyperlordosis, while some cases retain near-normal sagittal alignment.

Overall, increased extension moments and compensatory mechanisms play key biomechanical roles in the initiation and progression of AIS. Understanding these mechanisms may help refine orthotic strategies, improve sagittal correction, and support the development of unified 3D biomechanical principles for AIS management.

Figure and Table Legends

Figure 1. **Patient Selection Flowchart**

Figure 2. **Measurement and Key Anatomical Landmarks of Five Sagittal Segmental Radiographic Spinal Alignment Parameters (RSAPs)**

Figure 3. **Measurement and Key Anatomical Landmarks of the Three Sagittal Deviational Angles (SDAs):** (a) Sagittal Central Sacral Line (SCSL): a vertical line drawn from the midpoint of the S1 in the sagittal plane, (b) C4/5: the midpoint between the posterior-inferior corner of the C4 vertebral body and the posterior-superior corner of the C5 vertebral body, (c) T7/8: the midpoint between the posterior-inferior corner of the T7 vertebral body and the posterior-superior corner of the T8 vertebral body, and (d) L3/4: the midpoint between the posterior-inferior corner of the L3 vertebral body and the posterior-superior corner of the L4 vertebral body

Figure 4. **Illustrations and Radiographic Examples of the Seven Sagittal Misalignment Types with Sagittal Central Sacral Lines (red vertical lines):** (a) Type 1, and (b)-(g) Types 2-7 in solid lines, with Type 1 in blue dotted lines for comparison.

Table 1. **Seven Sagittal Misalignment Types and Their SDA Values and Sagittal Segmental RSAP Measurements:** This presents the means and standard deviations of five sagittal segmental RSAPs across the 7 newly identified sagittal misalignment patterns and results from non-parametric two-sample tests comparing Type 1 (minimal misaligned type) with other 6 sagittal misalignment types. Cells highlighted in grey indicate statistically significant differences with p-value < 0.05.

Table 2. **Characteristics of Sagittal Misalignment Types in AIS:** Description of sagittal misalignment characteristics for each type, based on sagittal segmental RSAP measurements and SDA values, as shown in Table 1.

References

1. Kane WJ. Scoliosis prevalence: a call for a statement of terms. Clin Orthop Relat Res. 1977;(126):43–6.
2. Reamy BV, Slakey JB. Adolescent idiopathic scoliosis: review and current concepts. Am Fam Physician. 2001;64(1):111–6.
3. Lowe TG, Edgar M, Margulies JY, Miller NH, Raso VJ, Reinker KA, et al. Etiology of idiopathic scoliosis: current trends in research. J Bone Joint Surg Am. 2000;82(8):1157–68.

4. Richards BS, Bernstein RM, D'Amato CR, Thompson GH. Standardization of criteria for adolescent idiopathic scoliosis brace studies: SRS Committee on Bracing and Nonoperative Management. *Spine (Phila Pa 1976)*. 2005;30(18):2068–75; discussion 2076–7.
5. Kuntz CI. Evaluation of spinal alignment: Part I—coronal alignment. *Contemp Neurosurg*. 2013;35(1):1.
6. Bernhardt M, Bridwell KH. Segmental analysis of the sagittal plane alignment of the normal thoracic and lumbar spines and thoracolumbar junction. *Spine (Phila Pa 1976)*. 1989;14(7):717–21.
7. Kapandji IA. The vertebral column as a whole. In: *The Physiology of the Joints: The Trunk and the Vertebral Column*. 2nd ed. Edinburgh: E. & S. Livingstone; 1970. p. 8–51.
8. Lenke LG, Betz RR, Harms J, Bridwell KH, Clements DH, Lowe TG, Blanke K. Adolescent idiopathic scoliosis: a new classification to determine extent of spinal arthrodesis. *J Bone Joint Surg Am*. 2001;83(8):1169–81.
9. Ovadia D. Classification of adolescent idiopathic scoliosis (AIS). *J Child Orthop*. 2013;7(1):25–8.
10. Glassman SD, Bridwell K, Dimar JR, Horton W, Berven S, Schwab F. The impact of positive sagittal balance in adult spinal deformity. *Spine (Phila Pa 1976)*. 2005;30(18):2024–9.
11. Abelin-Genevois K, Idjerouidene A, Roussouly P. Classification of sagittal alignment patterns in adolescent idiopathic scoliosis. *Eur Spine J*. 2021;30(6):1618–26. doi:10.1007/s00586-021-06772-w.
12. Jang SH, Davis KL, Thach SD. Current practice in orthotic treatment of AIS. *J Prosthet Orthot*. 2019;31(1):23–32. doi:10.1097/JPO.0000000000000221

13. American Academy of Orthotists and Prosthetists. Point of Consensus: Orthosis Biomechanics. *J Prosthet Orthot.* 2003;15(4S):S46–S48.
14. Rigo M, Negrini S, Weiss H, et al. SOSORT consensus paper on brace action: TLSO biomechanics of correction (investigating the rationale for force vector selection). *Scoliosis.* 2006;1(1):11.
15. de Mauroy J, Weiss H, Aulisa A, et al. 7th SOSORT consensus paper: conservative treatment of idiopathic and Scheuermann's kyphosis. *Scoliosis.* 2010;5:9.
16. Negrini S, Aulisa AG, Aulisa L, et al. 2011 SOSORT guidelines: orthopaedic and rehabilitation treatment of idiopathic scoliosis during growth. *Scoliosis.* 2012;7:3.
17. Bradford DS, Moe JH, Montalvo FJ, Winter RB. Scheuermann's kyphosis and roundback deformity: results of Milwaukee brace treatment. *J Bone Joint Surg Br.* 1974;56(4):740–58.
18. Ghandhari H, Hesarikia H, Ameri E, Noori A. Assessment of normal sagittal alignment of the spine and pelvis in children and adolescents. *Biomed Res Int.* 2013; 2013:912375.
19. La Maida GA, Zottarelli L, Mineo GV, Misaggi B. Sagittal balance in adolescent idiopathic scoliosis: radiographic study of spino-pelvic compensation after surgery. *Eur Spine J.* 2013;22(Suppl 6):S859–67.
20. Propst-Proctor SL, Bleck EE. Radiographic determination of lordosis and kyphosis in normal and scoliotic children. *J Pediatr Orthop.* 1983;3(3):344–6.
21. Stagnara P, De Mauroy JC, Dran G, Gonon GP, Costanzo G, Dimnet J, et al. Reciprocal angulation of vertebral bodies in a sagittal plane: approach to references for the evaluation of kyphosis and lordosis. *Spine (Phila Pa 1976).* 1982;7(4):335–42.

22. Vialle R, Levassor N, Rillardon L, Templier A, Skalli W, Guigui P. Radiographic analysis of the sagittal alignment and balance of the spine in asymptomatic subjects. *J Bone Joint Surg Am.* 2005;87(2):260–7.
23. Pearsaii DJ, Reid JG. Line of gravity relative to upright vertebral posture. *Clin Biomech (Bristol).* 1992;7(2):80-86. doi:10.1016/0268-0033(92)90019-Z
24. Castelein RM, Veraart BE. Idiopathic scoliosis: prognostic value of the profile. *Eur Spine J.* 1992;1(3):167–9.
25. Castelein RM, van Dieën JH, Smit TH. The role of dorsal shear forces in the pathogenesis of adolescent idiopathic scoliosis: a hypothesis. *Med Hypotheses.* 2005;65(3):501–8.
26. Kouwenhoven JW, Smit TH, van der Veen AJ, Kingma I, van Dieën JH, Castelein RM. Effects of dorsal versus ventral shear loads on the rotational stability of the thoracic spine: a biomechanical porcine and human cadaveric study. *Spine (Phila Pa 1976).* 2007;32(24):2545–50.
27. Schlösser TP, Colo D, Castelein RM. Etiology and pathogenesis of adolescent idiopathic scoliosis. *Semin Spine Surg.* 2015;27(1):2–8.
28. Roussouly P, Gollogly S, Berthonnaud E, Dimnet J. Classification of the normal variation in the sagittal alignment of the human lumbar spine and pelvis in the standing position. *Spine (Phila Pa 1976).* 2005;30(3):346–353. doi:10.1097/01.brs.0000152379.54463.65
29. Dickson RA, Lawton JO, Archer IA, Butt WP. The pathogenesis of idiopathic scoliosis: biplanar spinal asymmetry. *J Bone Joint Surg Br.* 1984;66(1):8–15.
30. Burwell RG. Aetiology of idiopathic scoliosis: current concepts. *Pediatr Rehabil.* 2003;6(3–4):137–70.

31. Masharawi Y, Rothschild B, Dar G, Peleg S, Robinson D, Been E, Hershkovitz I. Facet orientation in the thoracolumbar spine: three-dimensional anatomic and biomechanical analysis. **Spine**. 2004;29(16):1755–1763. doi:10.1097/01.BRS.0000134575.04084.EF
32. White AA III, Panjabi MM. *Clinical Biomechanics of the Spine*. 2nd ed. Baltimore, MD: Lippincott Williams & Wilkins; 1990.

Tables and Figures

Figure 1:

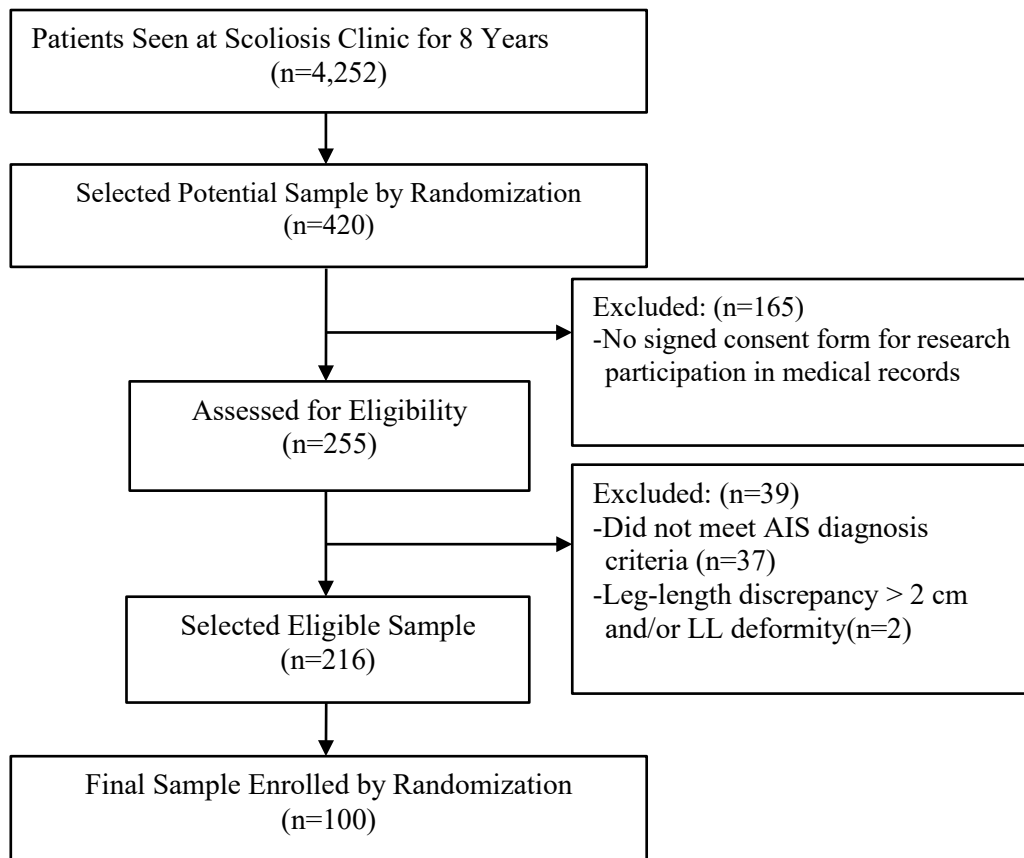


Figure 2:

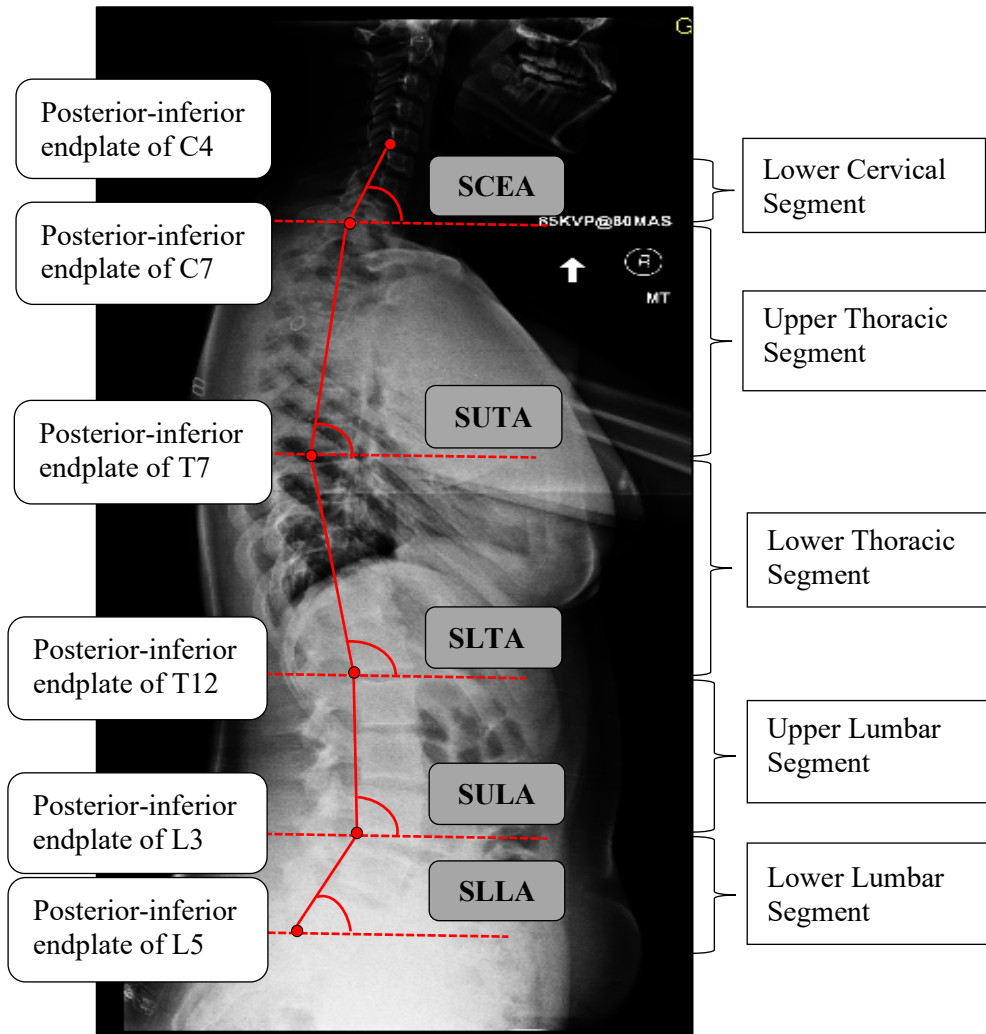


Figure 3:

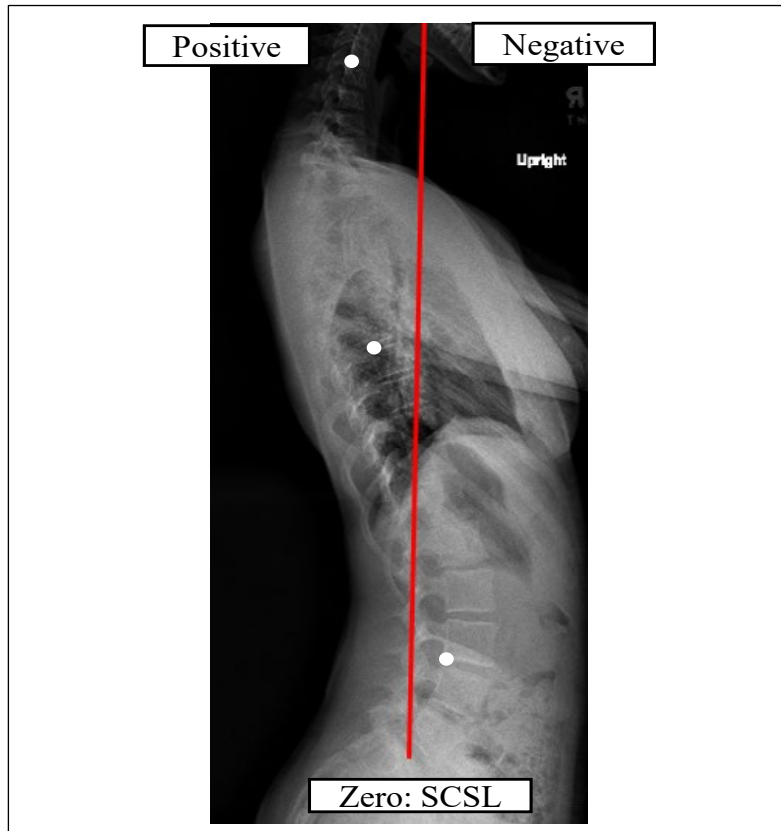


Figure 4:

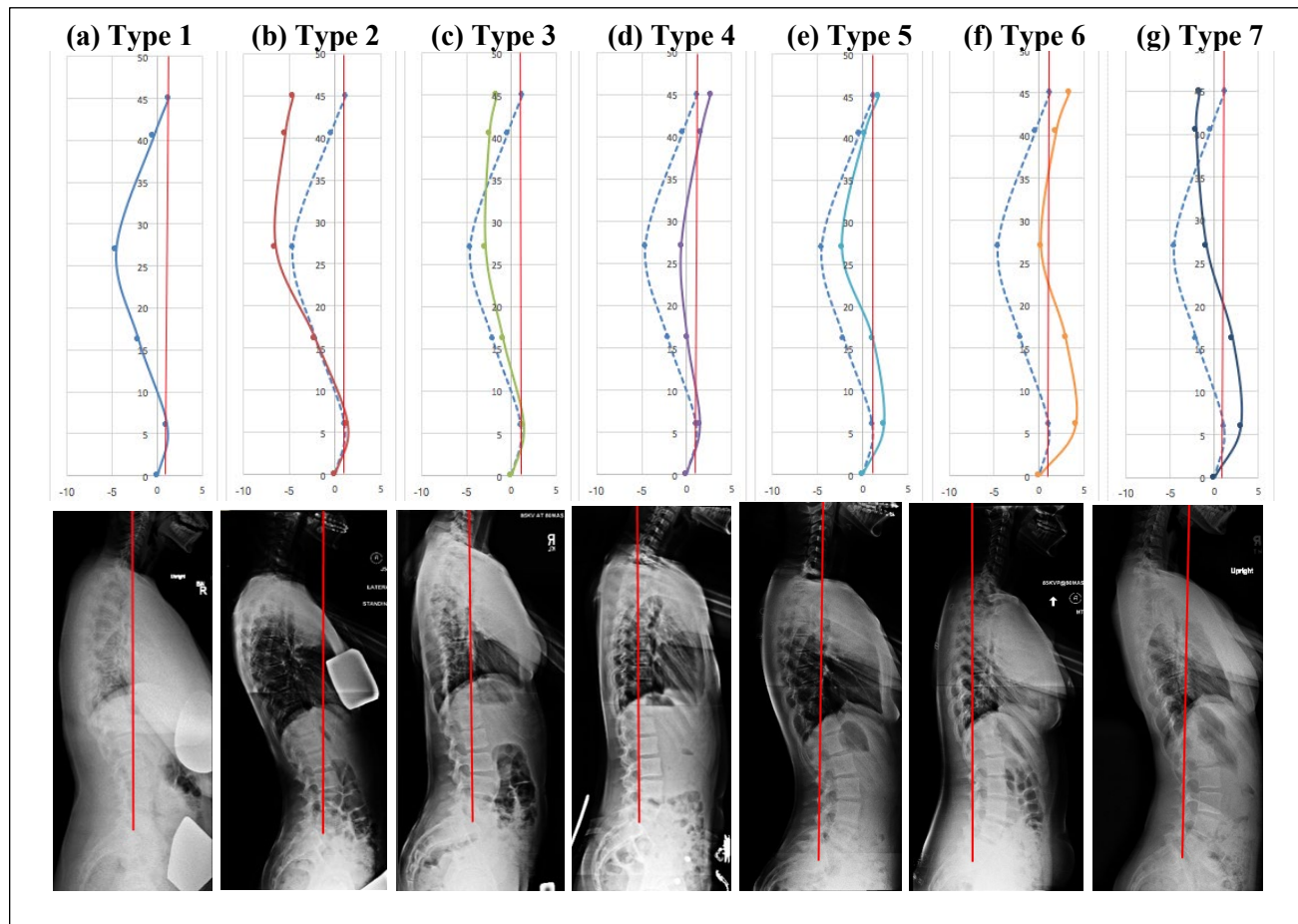


Table 1:

SDAs/ Sagittal Segmental RSAPs	Seven Sagittal Misalignment Patterns						
	Sagittal Segmental RSAPs: Mean \pm Std. Deviation (p = significance value, <0.05)						
	Type 1 (n= 16)	Type 2 (n= 34)	Type 3 (n= 23)	Type 4 (n= 7)	Type 5 (n= 7)	Type 6 (n= 9)	Type 7 (n= 4)
SAC4	0	+	+	-	0	-	+
SAT7	+	+	+	+	+	+	+
SAL3	0	0	0	0	-	-	-
SCEA	70.1 \pm 4.5	79.0 \pm 7.3 (p = .000)	79.9 \pm 6.9 (p = .000)	76.9 \pm 5.3 (p = .012)	70.9 \pm 5.4 (p = .579)	72.1 \pm 8.2 (p = .522)	84.8 \pm 7.1 (p = .002)
SUTA	72.9 \pm 3.3	85.5 \pm 7.2 (p = .000)	88.1 \pm 5.0 (p = .000)	80.9 \pm 2.9 (p = .000)	79.6 \pm 3.2 (p = .000)	82.7 \pm 3.8 (p = .000)	95.0 \pm 6.4 (p = .000)
SLTA	103.0 \pm 4.2	111.8 \pm 4.2 (p = .000)	100.4 \pm 5.4 (p = .128)	93.6 \pm 5.6 (p = .001)	107.6 \pm 4.7 (p = .033)	104.6 \pm 4.6 (p = .487)	105.5 \pm 2.4 (p = .437)
SULA	107.1 \pm 3.6	109.3 \pm 4.7 (p = .180)	102.7 \pm 3.1 (p = .000)	97.7 \pm 6.7 (p = .001)	96.9 \pm 4.9 (p = .000)	96.3 \pm 4.6 (p = .000)	95.3 \pm 1.0 (p = .000)
SLLA	80.1 \pm 5.3	77.0 \pm 6.6 (p = .100)	77.2 \pm 4.8 (p = .107)	76.1 \pm 3.8 (p = .154)	68.4 \pm 4.0 (p = .000)	55.7 \pm 5.6 (p = .000)	63.5 \pm 8.5 (p = .005)

Table 2:

Types	Sagittal segmental RSAP Measurements Compared to Natural Alignment	SDA Values	Characteristics
Type 1	Natural Alignment of All Five Segments	No C4 sagittal decompensation	Minimal misalignment type ; used as reference configuration
Type 2	Excessive posterior tilt of lower cervical, upper thoracic, and lower thoracic segments	Severe posterior C4 decompensation	Most severe cervicothoracic hyperextended type ; posterior tilting of the thoracic spine with severe thoracic hypokyphosis and pronounced posterior decompensation of the superior segments
Type 3	Excessive posterior tilt of lower cervical and upper thoracic segments; insufficient posterior tilt of upper lumbar segment	Posterior C4 decompensation	Severe thoracic hypokyphosis with cervical posterior decompensation; vertical straightening of the upper lumbar segment
Type 4	Excessive posterior tilt of lower cervical and upper thoracic segments; insufficient posterior tilt of lower thoracic and upper lumbar segments	Anterior C4 decompensation	Most vertically straightened type ; mild thoracic hypokyphosis with cervical anterior decompensation; straightening of upper lumbar and lower thoracic segments
Type 5	Excessive posterior tilt of upper and lower thoracic segments; insufficient posterior tilt of upper lumbar segment; excessive anterior tilt of lower lumbar segment	No C4 sagittal decompensation; significant anterior deviation of L3	Lumbar hyperlordosis with severe anterior tilt of the lower lumbar segment and vertical straightening of the upper lumbar and lower thoracic segments; mild thoracic hypokyphosis without cervical decompensation
Type 6	Excessive posterior tilt of upper thoracic segment; insufficient posterior tilt of upper lumbar segment; severe anterior tilt of lower lumbar segment	Anterior C4 decompensation; significant anterior deviation of L3	Most severe lumbar hyperlordotic type ; characterized by pronounced anterior tilt of the lower lumbar segment and vertical straightening of the upper lumbar segment; mild thoracic hypokyphosis with cervical anterior decompensation
Type 7	Excessive posterior tilt of lower cervical and upper thoracic segments; insufficient posterior tilt of upper lumbar segment; severe anterior tilt of lower lumbar segment	Severe posterior C4 decompensation; significant anterior deviation of L3	Combined cervicothoracic hyperextension and lumbar hyperlordotic type ; characterized by posterior tilting of the thoracic spine with severe thoracic hypokyphosis and marked posterior decompensation of the superior segments, along with pronounced anterior tilt of the lower lumbar segment and vertical straightening of the upper lumbar segment